

On the Theoretical Understanding of Nanocrystalline Soft Magnetic Materials

G. Herzer

Nanocrystalline structures offer a new opportunity for tailoring soft magnetic materials. The most prominent examples are devitrified glassy FeCuNbSiB alloys, which exhibit a homogeneous ultrafine grain structure of bcc FeSi, with grain sizes of typically 10 to 15 nm and random texture. Due to the small grain size, the local magnetocrystalline anisotropy is randomly averaged out by exchange interactions so that there is only a small anisotropy net effect on the magnetization process. Moreover, the structural phases present lead to low or vanishing saturation magnetostriction. Both the suppressed magnetocrystalline anisotropy and the low magnetostriction provide the basis for the superior soft magnetic properties comparable to those of Permalloys or near-zero magnetostrictive Co-base amorphous alloys, but at a higher saturation induction.

Keywords

magnetic anisotropy, nanocrystalline ferromagnets, saturation magnetostriction, soft magnetic materials

1. Introduction

NANOCRYSTALLINE materials are single-phase or multiphase polycrystals, the crystal size of which is in the nanometer range, typically 5 to 50 nm. They can be produced by processes such as compaction of nanometer-size powders, deposition techniques, or by crystallization from the amorphous state.

In terms of magnetic properties, fine particle systems, so far, have been mostly discussed as hard magnetic materials.^[1] The reduction of particle size is a well-known approach to subdividing the material into "single-domain" particles, which increases coercivity, H_c , toward a maximum controlled by the anisotropies present. Although it is known that H_c decreases for very small particles, the regime in which grain sizes are much smaller than the single-domain particle and domain wall sizes has remained relatively unexplored. Accordingly, the attempt in soft magnetic engineering has been to make the grain size as large as possible to obtain low coercivities and high permeabilities.^[2]

The situation began to change with amorphous, soft magnetic alloys^[3] and, in particular, has changed dramatically with the recent discovery of ultrafine crystalline Fe-base alloys exhibiting superior soft magnetic properties.^[4,5] The most prominent examples are devitrified glassy FeCuNbSiB alloys,^[4] which exhibit a homogeneous ultrafine grain structure of bcc FeSi, with typical grain sizes of 10 to 15 nm and random orientation. Further examples are devitrified glassy alloys based on CoNbB^[6] or FeZrB,^[7] Fe-*M*-C (*M* = Ti, Zr, Hf, Nb, or Ta) thin films,^[8] and multilayered structures like Fe/CoNbZr.^[9]

The present state of the art is shown in Fig. 1, in which the coercivity, H_c , of nanocrystalline Fe-base alloys has been plotted versus the average grain size together with data for amor-

phous and conventional polycrystalline soft magnetic materials.^[5] The $1/D$ dependence for large grain sizes ($D > 100 \mu\text{m}$) reflects the classical rule that good soft magnetic properties require very large grains. Lowest coercivities are also found for amorphous alloys (grain size on the order of atomic distances) and in the nanocrystalline FeCuNbSiB alloys for grain sizes $D < 15 \text{ nm}$. The initial permeability shows an analogous behavior being essentially inversely proportional to H_c . Obviously, the new nanocrystalline material fills the gap between amorphous metals and conventional polycrystalline alloys. The D^6 dependence of coercivity for grain sizes between about 10 and 40 nm moreover demonstrates how closely soft and hard magnetic behavior can be neighbored.

Nanocrystalline FeCuNbSiB alloys are of particular interest, because their soft magnetic properties are comparable to those of Permalloys or amorphous Co-base alloys, but at significantly higher saturation induction of typically $B_s \approx 1.2 \text{ T}$. Typical values are coercivities, H_c , of less than 10 mA/cm and initial permeabilities up to 100,000^[4] and higher. The key factor to tailor such superior soft magnetic properties is understanding magnetic anisotropies and how they can be controlled. In the simplest approach, the coercivity, H_c , is proportional to the anisotropy energy density, K , and the initial permeability is $\mu_i \propto 1/K$. Thus, the basic conditions for good soft magnetic properties generally are low or vanishing magnetic anisotropies of a few J/m³ only.

The major anisotropy contributions may be divided into (1) magnetocrystalline anisotropy, K_1 , related to the crystal symmetry, the easy axis of magnetization being determined by the crystal axis, and (2) magneto-elastic anisotropy, $K_\sigma \propto \lambda_s \cdot \sigma$, originating from internal or external mechanical stresses, σ , due to magnetostrictive coupling. The relevant material parameter is given by the saturation magnetostriction, λ_s .

The present article reviews the consequences of the nanocrystalline structure for these basic anisotropy contributions. The materials highlighted will be FeCuNbSiB alloys produced via crystallization from the amorphous state. The general features, however, also apply to other nanocrystalline magnetic materials.

G. Herzer, Vacuumschmelze GmbH, Hanau, Germany.

2. Magnetocrystalline Anisotropy

The magnetocrystalline anisotropy, K_1 , of bcc Fe-20Si, the constituent crystalline phase in the FeCuNbSiB alloys,^[13,14] is still about $K_1 = 8000 \text{ J/m}^3$.^[15] This value is by far too large to explain by itself the low coercivities and the high initial permeabilities observed for nanocrystalline materials. The key to understanding is to recognize the role of ferromagnetic exchange energy. Actually, the grain size in the nanocrystalline material is much smaller than the ferromagnetic exchange length:

$$L_{ex}^0 = (A/K_1)^{1/2} \quad [1]$$

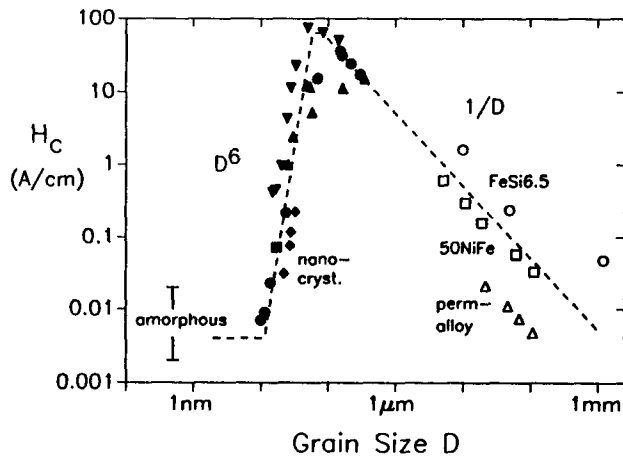
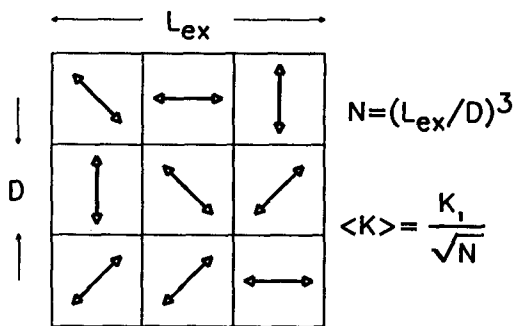


Fig. 1 Coercivity, H_c , versus grain size, D , for various soft magnetic metallic alloys. The nanocrystalline materials shown are FeNbSiB (closed triangles), FeCuNbSiB (closed circles),^[5] FeCuVSiB (diamonds),^[10] FeZrB (closed squares),^[7] and Fe-CoZr (reverse triangles).^[11] The data for the NiFe alloys (open squares and triangles) and Fe-6.5Si (wt%) (open circles) are from Ref 2 and 12, respectively.



(a)

where A denotes the exchange stiffness, which is about $L_{ex}^0 \approx 35 \text{ nm}$ for the present material. L_{ex}^0 represents the minimum scale within which the magnetic moments are forced to align parallel by exchange interaction. The domain wall width, for example, is typically $\delta_B = \pi \cdot L_{ex}$. Thus, magnetization cannot follow the randomly oriented easy axis of each individual grain. As a consequence, the effective anisotropy is an average of several grains and, thus, reduced in magnitude.

2.1 Grain Size Effect

To interpret the magnetic properties in the regime where the grain size is much smaller than the exchange length, the random anisotropy model originally proposed by Alben et al.^[16] for amorphous ferromagnets is used. The basic concept is shown in Fig. 2(a) and starts from an assembly of ferromagnetically coupled grains of size D with magnetocrystalline anisotropies K_1 oriented at random.

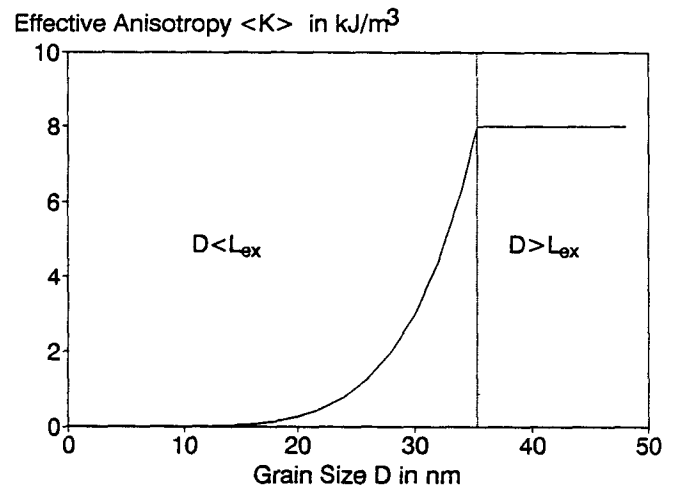
The effective anisotropy relevant to the magnetization process results from averaging over the $N = (L_{ex}/D)^3$ grains within the volume $V = L_{ex}^3$ of the exchange length. For a finite number, N , of grains, there will always be some easiest direction determined by statistical fluctuations. As a consequence, the resulting anisotropy density $\langle K \rangle$ is determined by the mean fluctuation amplitude of the anisotropy energy of the N grains, i.e.:

$$\langle K \rangle \approx \frac{K_1}{\sqrt{N}} = K_1 \left(\frac{D}{L_{ex}} \right)^{3/2} \quad [2]$$

In turn, the exchange length, L_{ex} , now is related self-consistently to the average anisotropy by substituting $\langle K \rangle$ for K_1 in Eq 1, i.e.:

$$L_{ex} = \sqrt{\frac{A}{\langle K \rangle}} \quad [3]$$

This renormalization of L_{ex} results from the counterplay of anisotropy and exchange energy: As magnetocrystalline an-



(b)

Fig. 2 (a) Schematic representation of the random anisotropy model. The arrows indicate the randomly fluctuating anisotropies. (b) Estimate of the effective anisotropy $\langle K \rangle$ for the randomly oriented bcc FeSi grains as a function of average grain size.

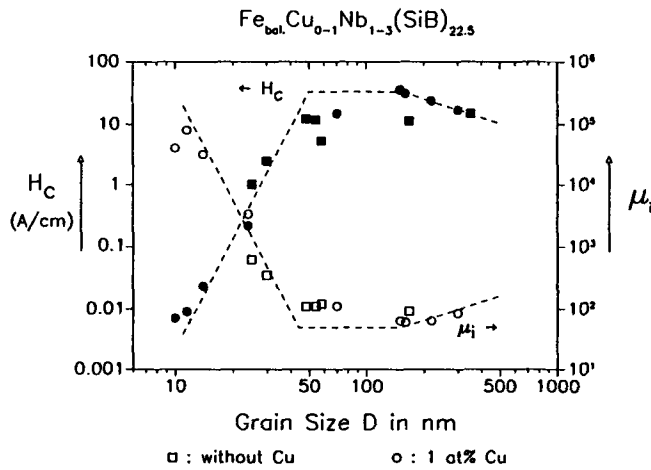


Fig. 3 Grain size dependence of coercivity, H_c (closed symbols), and initial permeability, μ_i (open symbols), in nanocrystalline $\text{Fe}_{74.5-x}\text{Cu}_x\text{Nb}_3(\text{SiB})_{22.5}$ alloys (circles: $x_{\text{Cu}} = 1$ at.%; squares: $x_{\text{Cu}} = 0$) annealed 1 h at different temperatures. The dashed lines show the variation H_c , $1/\mu_i \propto D^6$ below 40 nm and H_c , $1/\mu_i \propto 1/D$ above 150 nm.

isotropy is suppressed by exchange interaction, the scale on which exchange interactions dominate expands at the same time, and thus, the local anisotropies are averaged out even more effectively.

The combination of Eq 2 and 3 finally yields:

$$\langle K \rangle \approx \frac{K_1^4}{A^3} \cdot D^6 \quad (4)$$

which holds as long as the grain size D is smaller than the exchange length, L_{ex} . It should be noted that this result is essentially based on statistical and scaling arguments and, therefore, is not limited to the case of uniaxial anisotropies (as may be anticipated from Fig. 2a), but also holds for cubic or other symmetries.

An estimate of the averaged anisotropy, $\langle K \rangle$, as a function of the grain size, D , is shown in Fig. 2(b) for the material parameters of $\alpha\text{Fe-20Si}$ ($A \approx 10^{-11}$ J/m, $K_1 = 8$ kJ/m³). Obviously, grain sizes below about 20 nm are small enough to suppress the local magnetocrystalline anisotropy, K_1 , sufficiently. For grain sizes of $D = 10$ nm, for example, the average anisotropy is only $\langle K \rangle = 4$ J/m³, which is almost negligible compared to K_1 . High-resolution Kerr effect studies of nanocrystalline $\text{Fe}_{73.5}\text{Cu}_1\text{Nb}_3\text{Si}_{13.5}\text{B}_9$ indeed reveal very wide domain walls of about 2 μm thickness, indicative of the low effective anisotropy of the material.^[17]

Coercivity and initial permeability are closely correlated to the effective anisotropy $\langle K \rangle$ by:^[5]

$$H_c = p_c \frac{\langle K \rangle}{J_s} \approx p_c \frac{K_1^4}{J_s A^3} \cdot D^6 \quad (5)$$

$$\mu_i = p_\mu \frac{J_s^2}{\mu_o \langle K \rangle} \approx p_\mu \frac{J_s^2 \cdot A^3}{\mu_o K_1^4} \cdot 1/D^6 \quad (6)$$

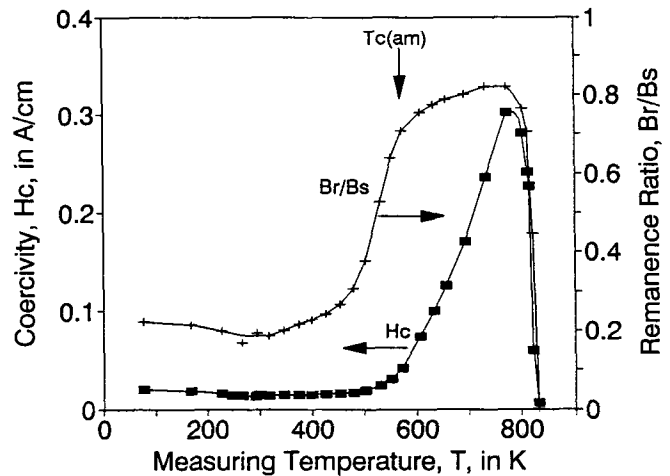


Fig. 4 Coercivity, H_c , and remanence to saturation ratio, B_r/B_s , of nanocrystalline $\text{Fe}_{73.5}\text{Cu}_1\text{Nb}_3\text{Si}_{13.5}\text{B}_9$ (annealed 1 h at 540 °C + 4 h at 350 °C in a transverse magnetic field) as a function of the measuring temperature ($f = 50$ Hz).

where p_c and p_μ are dimensionless prefactors close to unity. These relations, valid for the regime $D < L_{ex}^0$, were shown to hold both for domain displacement and rotational processes, i.e., they apply irrespective of the detailed mechanisms of the magnetization reversal.^[5]

The $D^{[6]}$ dependence is well reflected in the coercivity and permeability data for grain sizes below about 40 nm ($\approx L_{ex}^0$). Figure 3 supplements the permeability for some of the alloys shown in Fig. 1. Analysis of the experimental data yields for the prefactors $p_c \approx 0.13$ and $p_\mu \approx 0.5$, respectively. This compares reasonably well with the predictions of fine particle theory (e.g., $p_c = 0.64$ and $p_\mu = 0.33$ for cubic particles oriented at random).

If the grain size exceeds the exchange length, the magnetization process is determined by the full magnetocrystalline anisotropy K_1 . Accordingly, H_c and $1/\mu_i$ run through a maximum at $D \approx L_{ex}$. Finally, if the grain size exceeds the domain wall width, $\delta_B = \pi L_{ex}$, domains can be formed within the grains, and H_c and $1/\mu_i$ tend to decrease again according to the well-known $1/D$ -law.^[2,5]

2.2 Grain Coupling

The suppression of magnetocrystalline anisotropy requires that the randomly oriented grains are ferromagnetically coupled by exchange interaction. Consequently, if the exchange interaction is reduced, the local anisotropies will be less effectively averaged out (see Eq 4 and Ref 18), and the soft magnetic properties will degrade.

The exchange interaction between the bcc grains mainly occurs via the interfacial amorphous minority matrix in which the nanocrystallites are embedded.^[13,14,18] Hence, it is sensitive to the local magnetic moments there. Now, the thermomagnetic analysis shows^[18] that the interfacial component becomes paramagnetic at around 300 °C, i.e., far below the Curie temperature of the bcc grains ($T_C \approx 600$ °C). Thus, the exchange interaction between the crystallites is reduced with increasing

temperature and, finally, is largely interrupted at the Curie point of the intergranular phase. The latter leads to a significant increase of coercivity by more than one order of magnitude, as shown in Fig. 4. Simultaneously, the domain structure changes from wide domains to a pattern of small, irregular domains.^[17] The behavior described is essentially reversible, i.e., structural changes during the measurement can be largely ruled out.

Similar to the temperature dependence, the reduction of the magnetic moment in the interfacial phase by alloying, for example, too much Nb,^[19] may also lead to inferior soft magnetic properties.

The increase in coercivity with temperature, finally, unequivocally rules out superparamagnetic phenomena. This is important to note because thermal effects, i.e., the transition to superparamagnetism, also would provide a possible explanation for the decrease in coercivity for particle sizes much smaller than the domain wall width.^[20]

Figure 4 also includes the temperature dependence of the remanence to saturation ratio, B_r/B_s . The sample was annealed in a magnetic field that induced a macroscopic uniaxial anisotropy, K_u , of about 5 J/m^3 . The low value of B_r/B_s in the lower temperature regime indicates that this induced anisotropy controls the hysteresis loop (the measuring direction was perpendicular to the induced anisotropy axis), because the magnetocrystalline anisotropy is averaged out. However, for the higher temperatures where the exchange coupling is largely interrupted, the magnetocrystalline anisotropy takes over control of the hysteresis loop, because in this case, $K_1 \gg K_u$. This is the reason for the increase in the remanence to saturation ratio toward $B_r/B_s = 0.83$, which is the theoretical result for an assembly of noninteracting cubic particles oriented at random.^[21]

3. Saturation Magnetostriction

It is an additional highlight of the FeCuNbSiB alloys that the high positive saturation magnetostriction of $\lambda_s \approx +23 \times 10^{-6}$ decreases significantly with the formation of the nanocrystalline state.^[4] Figure 5(a) shows the evolution of saturation magnetostriction, λ_s , with annealing temperature. An example of the dependence on composition is shown in Fig. 5(b) for a $\text{Fe}_{73.5}\text{Cu}_1\text{Nb}_3\text{Si}_x\text{B}_{22.5-x}$ alloy series in the as-quenched amorphous state and after annealing 1 h at 540°C . Although λ_s is practically constant for the amorphous state, it depends sensitively on the Si content of the annealed nanocrystalline material, passing even through zero at $x_{\text{Si}} \approx 15.5$ at. %.

The behavior of λ_s can be understood from the two-phase nature of the material and the composition of the individual phases. The balance of magnetostriction among the bcc FeSi grains and the residual amorphous matrix yields:

$$\lambda_s \approx v_{\text{FeSi}} \cdot \lambda_s^{\text{FeSi}} + (1 - v_{\text{FeSi}}) \cdot \lambda_s^{\text{am}} \quad [7]$$

where v_{FeSi} denotes the crystalline volume fraction. Analysis of the experimental data shows that the magnetostriction of the crystalline bcc phase is negative ($\lambda_s^{\text{FeSi}} \sim -5 \times 10^{-6}$) and corresponds to that of conventional polycrystalline αFeSi of comparable composition.^[22] Accordingly, the residual amorphous matrix has a still relatively high positive magnetostriction ($\lambda_s^{\text{am}} \sim 10\text{--}25 \times 10^{-6}$) typical for amorphous Fe-base alloys enriched with B and Nb.

Thus, near-zero magnetostriction in nanocrystalline Fe-base alloys requires a large crystalline volume fraction with negative magnetostriction to compensate the high positive value of the amorphous Fe-base matrix. This is achieved either by a high Si content in the bcc grains, as in the present case, or

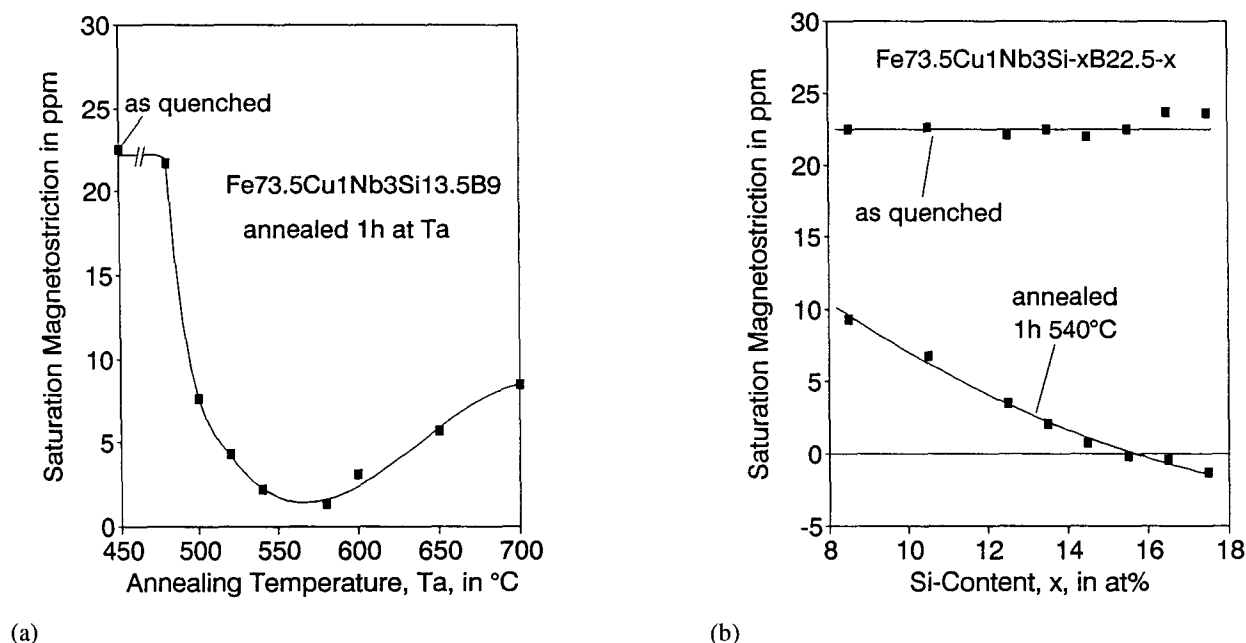


Fig. 5 Saturation magnetostriction, λ_s , of FeCuNbSiB alloys. (a) Influence of annealing temperature, T_a , for $\text{Fe}_{73.5}\text{Cu}_1\text{Nb}_3\text{Si}_{13.5}\text{B}_9$. (b) Influence of alloy composition for a $\text{Fe}_{73.5}\text{Cu}_1\text{Nb}_3\text{Si}_x\text{B}_{22.5-x}$ alloy series in the amorphous and nanocrystalline state.

if the grains consist of pure αFe ($\lambda_s \approx -4 \times 10^{-6}$), as in the case of FeZrB alloys.^[7]

Low saturation magnetostriction is essential to avoid magneto-elastic anisotropies arising from internal or external mechanical stresses. Accordingly, the decrease in magnetostriction on the formation of the nanocrystalline state is reflected in a simultaneous increase of initial permeability by about one order of magnitude.^[4,5] Still, the best soft magnetic properties are not necessarily found on the $\lambda_s \approx 0$ line, but for compositions where the total amount of magneto-elastic and magnetocrystalline anisotropy is minimized.^[13,23]

4. Conclusions

The basic mechanism for the soft magnetic properties of nanocrystalline ferromagnets is that the local magnetocrystalline anisotropies are randomly averaged out for grain sizes smaller than the ferromagnetic exchange length, similar to the case of amorphous alloys. Moreover, the phases formed on crystallization lead to low or vanishing saturation magnetostriction, which minimizes magneto-elastic anisotropies.

Both the low magnetocrystalline anisotropy and low or vanishing magnetostriction are the preconditions for superior soft magnetic properties. There are only a few alloy systems that exhibit this combination of properties: the Permalloys, Sendust, Mn-Zn-Ferrites, amorphous Co-base alloys, and now the nanocrystalline Fe-base alloys. Among these, the nanocrystalline alloys offer the highest saturation magnetization of about $J_s = 1.2$ to 1.3 T, which makes them an interesting candidate for soft magnetic applications.

As in other soft magnetic materials, magnetic field annealing allows variation in the shape of the hysteresis loop according to the demands of various applications.^[23,24] The nanocrystalline FeCuNbSiB alloys also exhibit a relatively high electrical resistivity of about $135 \mu\Omega\text{cm}$. Combined with the low ribbon thickness of typically $20 \mu\text{m}$, this yields a favorable frequency dependence of permeability and low eddy current losses up to frequencies of 100 kHz and more.^[24] In fact, the soft magnetic properties are very similar to those of amorphous, near-zero magnetostrictive Co-base alloys. The advantages, however, are a higher saturation induction and a significantly better thermal stability of the soft magnetic properties. There is no doubt that nanocrystalline Fe-base alloys will supplement the spectrum of existing soft magnetic materials in the near future. Possible applications already envisaged are tape-wound cores for common mode chokes, saturable reactors, high-frequency transformers, and magnetic heads.

References

1. F.E. Luborsky, High Coercive Materials, *J. Appl. Phys.*, Vol 32, 1961, p 171S-183S
2. F. Pfeiffer and C. Radeloff, Soft Magnetic Ni-Fe and Co-Fe Alloys—Some Physical and Metallurgical Aspects, *J. Magn. Magn. Mat.*, Vol 19, 1980, p 190-207
3. R. Boll and H.R. Hilzinger, Comparison of Amorphous Materials, Ferrites and Permalloys, *IEEE Trans. Magn. Mag.*, Vol 19, 1983, p 1946
4. Y. Yoshizawa, S. Oguma, and K. Yamauchi, New Fe-Based Soft Magnetic Alloys Composed of Ultrafine Grain Structure, *J. Appl. Phys.*, Vol 64, 1988, p 6044-6046
5. G. Herzer, Grain Size Dependence of Coercivity and Permeability in Nanocrystalline Ferromagnets, *IEEE Trans. Magn.*, Vol 26, 1990, p 1397-1402
6. R.C. O'Handley, J. Megusar, S.-W. Sun, Y. Hara, and N.J. Grant, Magnetization Process in Devitrified Glassy Alloy, *J. Appl. Phys.*, Vol 57, 1985, p 3563-3565
7. K. Suzuki, A. Makino, N. Kataoka, A. Inoue, and T. Matsumoto, High Saturation Magnetization and Soft Magnetic Properties of bcc Fe-Zr-B and Fe-Zr-B-M (M = Transition Metal) Alloys with Nanoscale Grain Size, *Mater. Trans. JIM*, Vol 32, 1991, p 93-102
8. N. Hasegawa, M. Saito, A. Kojima, A. Makino, Y. Misaki, and T. Watanabe, Crystallization Behaviour of Fe-M-C (M = Ti, Zr, Hf, V, Nb, Ta) Films, *J. Magn. Soc. Jpn.*, Vol 14, 1990, p 319-322
9. F. Dirne, F. den Broeder, J. Toolboom, H. de Wit, and C. Witmer, Soft-Magnetic Properties and Structures of Fe/CoNbZr Multilayers, *Appl. Phys. Lett.*, Vol 53, 1988, p 2386-2388
10. T. Sawa and Y. Takahashi, Magnetic Properties of FeCu (3d Transition Metals) SiB Alloys with Fine Grain Structure, *J. Appl. Phys.*, Vol 67, 1990, p 5565-5567
11. H.-Q. Guo, T. Reininger, H. Kronmüller, M. Rapp, and V.H. Skumrev, Magnetism and Microstructure in Nanocrystalline Fe-CoZr Ferromagnets, *Phys. Stat. Sol. (a)*, Vol 127, 1991, p 519-527
12. K.I. Arai, H. Tsutsumitake, and K. Ohmori, Grain Growth of Rapid Quenching High Silicon-Iron Alloys, *IEEE Trans. Magn. Mag.*, Vol 20, 1984, p 1463-1465
13. G. Herzer, "Magnetism and Microstructure of Nanocrystalline Fe-base Alloys," Proc. Int. Symp. 3d Transition-Semi Metal Thin Films, Jpn. Soc. Promotion of Science, 131 Committee (Thin Films), Sendai, Japan, 1991, p 130-139
14. K. Hono, K. Hiraga, Q. Wang, A. Inoue, and T. Sakurai, The Microstructure of a $\text{Fe}_{73.5}\text{Cu}_1\text{Nb}_3\text{Si}_{13.5}\text{B}_9$ Nanocrystalline Soft Magnetic Material, *Acta Metall. Mater.*, Vol 40, 1992, p 2137-2147
15. H. Gengnagel and H. Wagner, Magnetfeldinduzierte Anisotropie an FeAl- und FeSi-Einkristallen, *Z. Angew. Physik*, Vol 8, 1961, p 174-177, in German
16. R. Alben, J.J. Becker, and M.C. Chi, Random Anisotropy in Amorphous Ferromagnets, *J. Appl. Phys.*, Vol 49, 1978, p 1653-1658
17. R. Schäfer, A. Hubert, and G. Herzer, Domain Observation on Nanocrystalline Material, *J. Appl. Phys.*, Vol 69, 1991, p 5325-5327
18. G. Herzer, Grain Structure and Magnetism of Nanocrystalline Ferromagnets, *IEEE Trans. Magn.*, Vol 25, 1989, p 3327-3329
19. Y. Yoshizawa and K. Yamauchi, Magnetic Properties of Fe-Cu-M-Si-B (M = Cr, V, Mo, Nb, Ta, W) Alloys, *Mater. Sci. Eng.*, Vol A133, 1991, p 176-179
20. E. Kneller, in *Magnetism and Metallurgy*, A.E. Berkowitz and E. Kneller, Ed., Academic Press, 1969, p 365
21. S. Chigazumi, *Physics of Magnetism*, R.E. Krieger Publishing, Malabar, FL, 1986, p 248
22. T. Yamamoto, *The Development of Sendust and Other Ferromagnetic Alloys*, Komiyama Printing, Chiba, Japan, 1991, p 26
23. G. Herzer, Nanocrystalline Soft Magnetic Materials, *J. Magn. Magn. Mat.*, Vol 112, 1992, p 258-262
24. Y. Yoshizawa and K. Yamauchi, Effects of Magnetic Field Annealing on Magnetic Properties in Ultrafine Crystalline Fe-Cu-Nb-Si-B Alloys, *IEEE Trans. Magn.*, Vol 25, 1989, p 3324-3326